Cross-sectional Study

ANNALS OF MEDICINE & SURGERY

OPEN

Computed tomographic assessment of risk of anterior skull base injury of adult patients in tertiary care centre: a cross-sectional study

Shailendra Katwal, MD[a,*], Ravi Ranjan Kumar, MD[e], Mukhtar Alam Ansari, PhD[b], Sundar Suwal, MD[c], Prasoon Ghimire, MD[d]

Background and objectives: Functional endoscopic sinus surgery (FESS) carries the risk of anterior skull base injury. Understanding computed tomography of the paranasal sinuses (CT PNS) and anatomical variations is crucial before surgery. Several classifications, including Kero's, Gera's, and Thailand-Malaysia-Singapore (TMS), assess the risk of skull base injury. The objective was to determine the risk of anterior skull base injury using CT PNS in adult patients.

Methods: A study of 188 patients with head and paranasal sinus pathologies used CT scans to measure olfactory fossa depth, the angle between lamina papyracea and horizontal plane, and the distance from the orbital rim to the cribriform plate. Variations were classified using Kero's, Gera's, and TMS classifications.

Results: The study involved 188 individuals aged 18–85, with OF depths ranging from 0.1 to 0.52 cm. Kero's Class I was observed in 82.44% and 81.38% of individuals, while distances from orbital floor to cribriform plate and ethmoidal roof ranged from 1.37 to 2.93 cm. TMS Type I was observed in all individuals, and the angle between lateral lamella of the cribriform plate and cribriform plate ranged from 34° to 85°. Gera's Class II was observed in 77.12% and 84.57% of individuals.

Conclusion: CT PNS provides important anatomical information for assessing the risk of skull base injury during FESS. Kero's, Gera's, and TMS classifications can be utilized to evaluate this risk. The study findings provide insights into the variations in olfactory fossa depth, distance measurements, and angle, which can aid in preoperative planning and reducing complications during FESS in Nepalese populations.

Keywords: CT PNS, Gera, Kero's, Skull base injury, TMS classification

Introduction

The ethmoid sinuses represent intricate anatomical entities that are juxtaposed with critical structures including the orbit, dura mater, and optic nerve[1]. Attaining a comprehensive understanding of the paranasal architecture and recognizing the prevalence of asymmetry in the ethmoidal fovea hold paramount significance for endoscopic surgeons, as these factors play a pivotal role in averting potential complications[2]. Mishaps during endoscopic ethmoid surgery, wherein adjacent structures are inadvertently harmed, can result in adverse outcomes such as cerebrospinal fluid leakage, orbital impairment, and haemorrhage. In instances of profound injury, there exists the possibility of direct penetration trauma affecting the dura mater, culminating in grave intracranial and intracerebral ramifications. It is noteworthy that the cribriform plate and the apex of the ethmoid sinus emerge as the most frequently afflicted sites within the anterior cranial fossa[3].

Consideration of ethmoidal fovea asymmetry holds notable implications in the assessment of computed tomography (CT) scans before endoscopic sinus surgery (EES)[4]. Research findings have elucidated disparities in the vertical dimensions of the ethmoidal roof, with the right side frequently manifesting a lower position in contrast to the left side. This anatomical variability predisposes right-sided interventions to heightened complications

HIGHLIGHTS

- This study utilized computed tomography scans to assess the risk of anterior skull base injury during sinus surgery.
- Measurements and classifications of anatomical features such as the olfactory fossa depth and ethmoid roof slope were conducted.
- The findings offer important insights for surgeons in evaluating the risk of complications and improving preoperative planning in sinus surgeries.

[a]Department of Radiology, Dadeldhura Subregional Hospital, Dadeldhura, [b]Department of Radiology, National Medical College, Birgunj, [c]Department of Radiology, Maharajgunj Medical College, Kathmandu, [d]Department of Radiology, Dhaulagiri Hospital, Baglung, Nepal and [e]Department of Radiology, Ruby General Hospital, Kolkata, India

Sponsorships or competing interests that may be relevant to content are disclosed at the end of this article.

*Corresponding author. Address: Department of Radiology, Dadeldhura Subregional Hospital, Dadeldhura, Tufandada 10300, Nepal. Tel.: +977 984 914 9630. E-mail: shailendrakatwal@gmail.com (S. Katwal).

Annals of Medicine & Surgery (2023) 85:5892–5898

Received 13 July 2023; Accepted 17 September 2023

Supplemental Digital Content is available for this article. Direct URL citations are provided in the HTML and PDF versions of this article on the journal's website, www.lww.com/annals-of-medicine-and-surgery.

Published online 2 October 2023

http://dx.doi.org/10.1097/MS9.0000000000001362

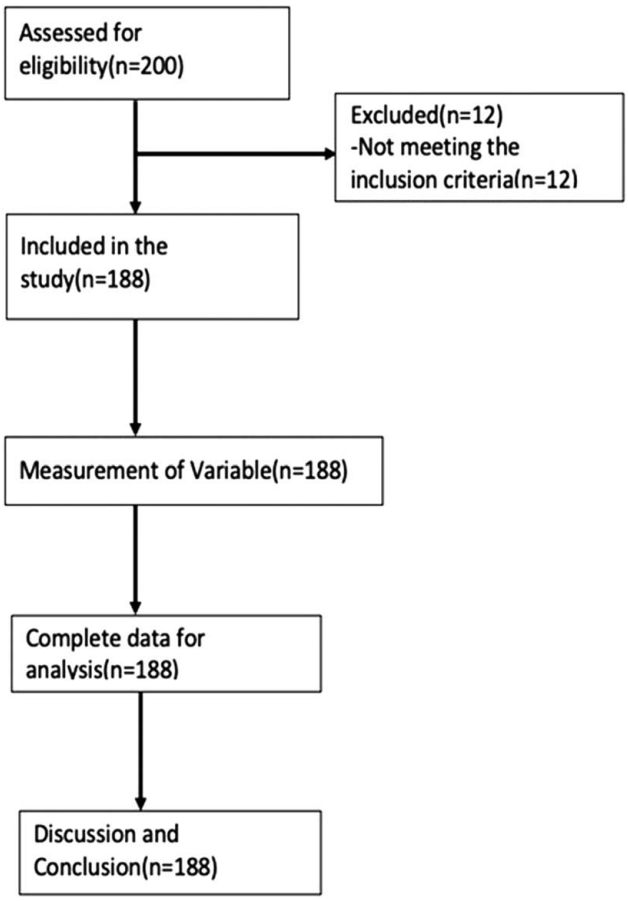

Figure 1. Flow diagram of the patient who underwent computed tomography (CT) head and CT of the paranasal sinuses in Tertiary care centre.

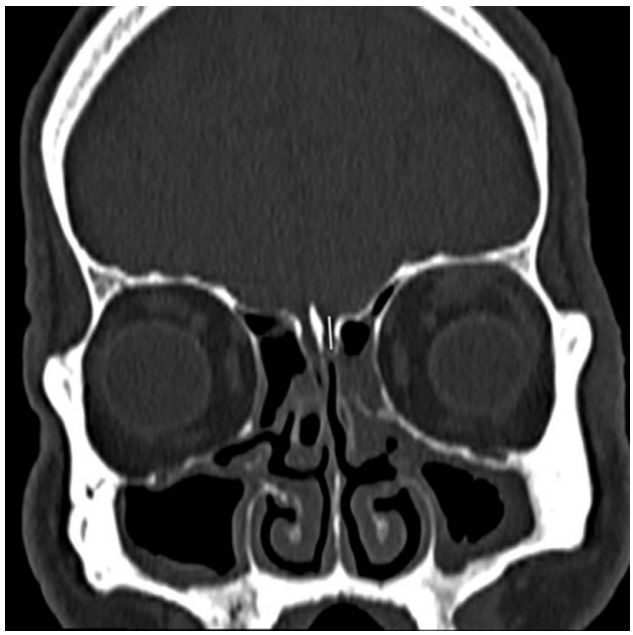

Figure 2. Depth of the cribriform plate, measured as the vertical height of the olfactory fossa in the computed tomography coronal plane.

compared to their left-sided counterparts[5]. Specifically, instances of cerebrospinal fluid leakage during ethmoidectomy on the right side, particularly when performed by right-handed surgeons, have been associated with the potentially awkward positioning of the surgeon[6].

Evaluation of the olfactory fossa (OF)'s depth and the classification framework introduced by Keros in 1962 are also germane considerations when assessing the risk of iatrogenic injury during fronthoethmoidal surgery. Keros categorized the OF into three distinct types based on their depth: Type I (1–3 mm), Type II (4–7 mm), and Type III (8–16 mm)[7]. Empirical evidence underscores the prevalence of Keros Type II, followed by Type I. Conversely, the occurrence of Keros Type III is less common, with respective incidences of 15.2% and 38%[8]. Notably, Keros Type III assumes a heightened vulnerability to iatrogenic injury during fronthoethmoidal procedures due to the extended length of its lateral lamella[9].

The point where the anterior ethmoidal artery (AEA) enters the OF via the lateral lamella is known for its thin anatomical structure, making it prone to injury and possible cerebrospinal fluid leaks. The AEA's path through the ethmoid sinus increases susceptibility to trauma, especially with a low angle or flattened contour. AEA damage can cause significant bleeding and lead to orbital haematoma due to the artery retracting into the orbit[10]. Practitioners performing endoscopic procedures must exercise caution when dealing with Keros Type I cases, given their heightened asymmetries, reduced ethmoidal roof elevation, and distinct characteristics of the AEA, in comparison to Keros Type III presentations, which are comparatively rare.

Further refinement of the risk assessment for anterior skull base injury is facilitated by alternative classification methodologies, such as Gera's classification and the recently formulated Thailand-Malaysia-Singapore (TMS) classification. Gera's classification scrutinizes the angle established by the lateral lamella of the cribriform plate and the continuation of the horizontal plane traversing through the cribriform plate[11]. The TMS classification, on the other hand, employs metrics such as the distances from the orbital floor (OrF) to the cribriform plate (CP) and from the orbital floor to the ethmoidal roof (ER) to delineate risk categories into three types: Type I (low risk), Type II (moderate risk), and Type III (high risk)[12].

Numerous investigations have delved into the assessment of the peril associated with anterior skull base injury using diverse categorization methodologies, notably Keros' classification. Investigations conducted in Nepal, India, and Egypt have unveiled divergences in the prevalence of different Keros types across distinct populations[13–15].

The Keros classification system has limitations in accurately determining intracranial penetration vulnerability due to cranial structure inclination. Gera's and TMS classifications provide supplementary tools to enhance existing systems, aiding surgeons in selecting appropriate micro instruments for ESS procedures[12].

CT plays a crucial role in evaluating sinonasal pathologies and the characterization of paranasal sinus anatomy. Coronal CT images are particularly important for identifying anatomical structures with significant variability. These images help identify potential hazards during endoscopic nasal surgeries, particularly in the frontoethmoidal region. CT imaging provides anatomical guidance, minimizing patients' postoperative complications and

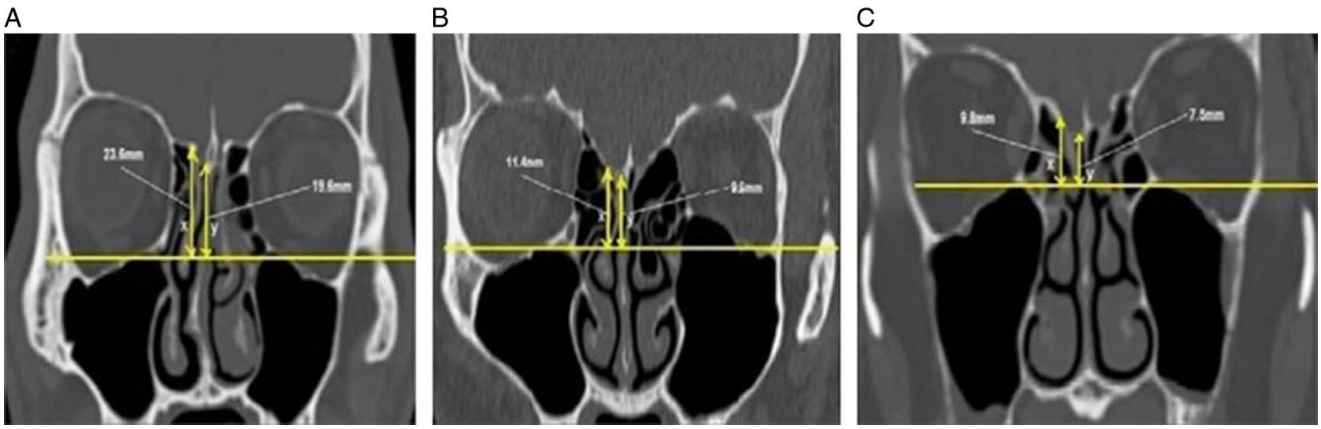

Figure 3. Computed tomography of the paranasal sinuses coronal section showing the three types of Thailand-Malaysia-Singapore classification. (A) is Type 1 (low risk) where both OF-CP and OF-ER are 10 mm and above, (B) is Type 2 (moderate risk) where either OF-CP or OF-ER is less than 10 mm and (C) is type 3 (high risk) where both OF-CP and OF-ER are less than 10 mm[12].

enhancing the overall patient experience[16]. MRI imaging is employed for suspected intracranial involvement of sinonasal malignancy and instances of uncertain anterior skull base engagement on CT[17].

ESS has improved complications compared to conventional methods, but accurate risk assessment is crucial. This study uses multiple categorization systems like Keros' and Gera's to examine variability and potential hazards in anterior skull base injuries in Nepal. The novel TMS classification system contributes to a more comprehensive understanding of this critical medical research area.

Methodology

Study design

The study used a quantitative observational cross-sectional study to assess the risk of anterior cranial fossa injury in adult patients. The study population consisted of 188 patients who underwent CT Head and CT of the paranasal sinuses (CT PNS) examinations at the Department of Radiology and Imaging in a tertiary health centre (Fig. 1). The study was started after approval by the Institutional Review Committee with reference number 236/(6–11)E^2/077/078. This study was conducted following the Strengthening the Reporting of Observational Studies in Epidemiology (STROBE) guideline. A complete STROBE 2016 checklist has been provided as a Supplementary File[18], Supplemental Digital Content 1, http://links.lww.com/MS9/A266. Our study is in accordance with the Declaration of Helsinki. The study also follows the Strengthening the reporting of cohort, cross-sectional and case-control studies in surgery (STROCSS 2021)[19], Supplemental Digital Content 2, http://links.lww.com/MS9/A267.

Sample size

The researchers used probability sampling to select the sample, which was determined using the formula.

$$\text{Sample size(n)} = Z^2pq/d^2$$

where Z is the z-value corresponding to a 95% confidence level ($Z = 1.96$), p is the estimated proportion of patients at moderate to high risk of anterior skull base injury based on a similar study by Bista and colleagues (14%), q is 1-p (proportion in the target population not having the particular characteristics), and d is the minimum allowable deviation or error of the estimate (5%). The calculated sample size was 185 patients. We studied 188 patients.

Table 1

Demographic profile of the patients who underwent CT head and paranasal sinus

Characteristics	Number, *n* (%)
Sex	
Male	116 (61.7)
Female	72 (38.29)
Age	
> 60 years	39 (20.74)
50–59 years	26 (13.82)
40–49 years	30 (15.95)
30–39 years	38 (20.21)
< 30years	55 (29.25)

CT, computed tomography.

Table 2

Distance measurement for orbital floor (OrF) to cribriform plate (CP) and orbital floor to ethmoidal roof (ER)

Distance from OrF to ER			
	Right side (cm)	Left side (cm)	*P* value (paired *t*-test)
Males	2.20 ± 0.30	2.23 ± 0.26	**0.00**
Females	2.15 ± 0.32	2.17 ± 0.28	0.51
Overall	2.19 ± 0.30	2.21 ± 0.27	0.49
Distance from OrF to CP			
Males	1.90 ± 0.29	1.91 ± 0.28	0.94
Females	1.85 ± 0.29	1.87 ± 0.28	0.49
Overall	1.88 ± 0.29	1.90 ± 0.28	0.50

Statistically significant *P* value in bold.

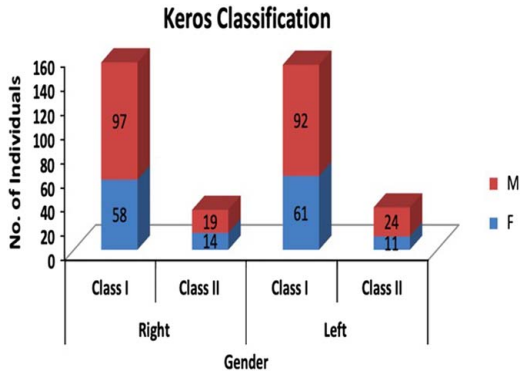

Figure 4. Frequency of study population according to Kero's classification.

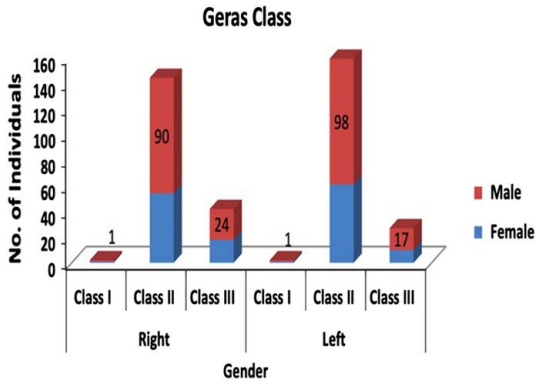

Figure 5. Frequency of study population according to Gera's classification.

The study encompassed adults aged 18 and above who underwent CT scans of the PNS and head from January 2021 to November 2021. Exclusions comprised patients with pathologies of the ethmoidal roof, anterior skull base, or medial orbit, those who had undergone skull base or paranasal sinus surgery, and cases with suboptimal CT images due to motion artifacts.

Variables examined included age, sex, OF depth bilaterally, the angle between the lateral lamella of the cribriform plate and a horizontal plane through the cribriform plate bilaterally, and the distance from the orbital floor to the cribriform plate and ethmoidal roof bilaterally. These variables were assessed to determine the risk of anterior cranial fossa injury in the studied population.

Tools and techniques for data collection

This study utilized a Siemens SOMATOM Definition AS+ CT machine with specified imaging parameters for head and paranasal sinus scans. Measurements were taken using bone view images and coronal reformation. Parameters assessed included OF depth (Fig. 2), angle between lateral lamella and horizontal plane, distance from orbital floor to cribriform plate, and orbital floor to ethmoidal roof distance (Fig. 3). Participant selection adhered to inclusion and exclusion criteria, with each participant providing written informed consent.

Trained radiologists directly measured variables on CT consoles to minimize missing data, ensuring real-time collection and reduced retrospective retrieval, enhancing study completeness. Collected data were entered into Microsoft Excel 2016 and IBM SPSS Statistics version 23. Frequency (%) represented discrete data, while mean ± SD represented categorical data. Uniform techniques were employed for measurements to prevent bias, and regular data reviews were conducted.

Although not directly involved in the study design, patients will receive the study's findings, benefitting from improved safety and effectiveness of functional ESS (FEES). Healthcare professionals will also be informed, contributing to enhanced surgical practices.

Results

This study included 188 patients meeting inclusion criteria, aged 18–85 years (mean age 42.7 ± 18.1 years). Most participants were male (61.70%), with the remaining being female (Table 1). OF depth was measured, showing no significant difference between the right and left sides (Table 2). Kero's classification showed more class I on the right and class II on the left, with no gender-based statistically significant differences (Fig. 4).

The study's findings indicate a range of distances between the OrF and the CP on both the right and left sides, with no significant difference between the two sides (Table 2). Distances between the OrF and CP had no significant difference between the sides, measuring 1.88 ± 0.29 cm (right) and 1.9 ± 0.28 cm (left). Distances between the OrF and ER had a significant difference in males ($P < 0.05$), measuring 2.19 ± 0.30 cm (right) and 2.21 ± 0.27 cm (left) (Table 2). These measurements are valuable for assessing anterior skull base injury risk during surgery. All subjects were TMS Type I, indicating a low risk.

The angle between lateral lamella of the cribriform plate (LLCP) and CP horizontal plane ranged from 34° to 85° (right) and 29° to 87° (left), with mean angles of 54.86° ± 11.54° (right) and 56.46° ± 11.06° (left). A significant angle difference was found between the females' left and right sides. Gera's classification showed most had class II on the left, and class III was less common with higher percentages on the right (Fig. 5).

Depth of cribriform showed a weak positive correlation with OF-CP ($r = 0.19$, $P < 0.05$). However, there was no significant correlation seen between depth of cribriform and OF-ER ($r = 0.12$, $P = 0.09$). The degree of angle formed by the lateral lamella of the CP and the continuation of the horizontal plane passing through the CP showed a weak positive correlation with OF-ER ($r = 0.17$, $P < 0.05$) while no significant correlation was seen with OF-CP ($r = 0.07$, $P = 0.35$) and depth of cribriform ($r = 0.33$, $P = 3.3$) (Table 3). Most of the patients were classified as Keros type I, TMS type I and Gera class II. There was no significant correlation seen between Keros and TMS classification ($P > 0.05$) (Table 4) as well as Gera and TMS classification ($P > 0.05$) (Table 5). Keros and Gera classification showed significant correlation on the right-sided measurements ($P < 0.05$) while no significant correlation seen in the left-sided measurements ($P = 0.2$) (Table 6).

Discussion

FESS is a minimally invasive technique enabling direct visualization for sinus air cell and ostia opening. CT significantly aids in evaluating sinonasal diseases and paranasal sinus anatomy. Coronal CT images serve as vital anatomy maps, revealing

Table 3

Correlation between the depth of cribriform, orbital floor to ethmoid roof height, orbital floor to cribriform plate height and angle between the lateral lamellae of cribriform plate and horizontal line passing through the cribriform plate (assessed using Pearson correlation, r value)

	Depth of cribriform	OF-ER[a]	OF-CP[b]	Angle
Depth of cribriform	1	0.12 ($P=0.09$)	0.19 ($P=0.009$)	0.33 ($P=3.3$)
OF-ER[a]	0.12 ($P=0.09$)	1	0.95 ($P=1.9$)	0.17 ($P=0.018$)
OF-CP[b]	0.19 ($P=0.009$)	0.95 ($P=1.9$)	1	0.07 ($P=0.35$)
Angle	0.33 ($P=3.3$)	0.17 ($P=0.018$)	0.07 ($P=0.35$)	1

[a]OF-ER: Distance from orbital floor to Ethmoid roof.
[b]OF-CP: Distance from Orbital floor to Cribriform plate.

inter-individual variability and guiding endoscopic nasal surgery planning to avoid complications.

Murthy *et al.*[20] investigated OF depth distribution based on Keros classification in 100 patients above age 10 in a rural tertiary hospital. They found OF depth ranged from 1 to 5.2 mm, with mean depths of 3.03 ± 1 mm on the right and 3.09 ± 0.9 mm on the left. They concluded that type II is the most common Keros type prevalent followed by type I Keros, and the least prevalent is type III Keros in the studied population. Our study, however, noted Keros Class I as the most common, followed by Types II and III. They identified 23 patients with asymmetrical OF and 77% with symmetrical fossa. Our study did not find significant OF symmetry differences between sides ($P > 0.05$).

In regards to the prevalence of depth of OF based on Kero's classification, our study showed similar findings to those conducted by Shreshtha *et al.*,[14] who found that Keros' type I was the most common (86.1%). Their study observed that the OF's right side was deeper in males, while in females, the left side was deeper. Overall, the right side was deeper in 52 patients (51.5%). However, our study found no statistically significant difference in the depths of the OF between the two sides.

Elwany *et al.*[21] observed dimensions for the depth of the OF, the length and angulation of the lateral lamella of the cribriform plate, and the height of the ethmoid roof in 300 adult males and females. The most common Keros type was type 2 (67.72%), followed by type 3 (22.28%), and type 1 (10%). However, our study showed that Keros Class I was the commonest type in both males and females.

Erdogan *et al.*[20] showed asymmetry in paranasal sinus CT images of Turkish patients without sinusitis in the ethmoid roof. They found lateral lamella heights of 5.78 mm on the right and 5.98 mm on the left, with type 2 being the most common type. This differed from our study which showed type I to be commonest and type III to be least common.

Mishra *et al.*[22] investigated the prevalence of dangerous ethmoid by analyzing computed tomography scans of 50 patients with chronic sinusitis undergoing endoscopic sinus surgery. Based on Kero's classification, they found that type II was the most prevalent type and type I the least common type. Costa *et al.*[23] investigated the OF according to the Keros classification using cone beam CT on the scans of 174 healthy patients. They found that the most prevalent Keros classification was type II (65.52%), followed by type III (20.69%) and type I (13.79%). Their results were different from our study observed with type I being most prevalent and type III being the least common. Similar to our study, no significant differences were found in the right side and left side of Kero's classification by Cosata and colleagues.

Moradi *et al.*[24] found that Keros type II was the most common ethmoid roof variation in 600 patients over 18 years old, with mean LLCP heights of 4.17 ± 1.69 mm for the right and left sides. These variations were independent of age and gender.

Babu *et al.*[15]measured variations in the depth of OF and categorize the Kerala population as per Keros classification using CT in Coronal PNS CT scan studies of 1200 patients. They found that the mean depth of OF was 5.26 ± 1.69 mm, with statistically significant variance seen in the mean depth of OF between males and females but not between the right and left sides. This finding was different from our study in terms of prevalence; however, regarding the statistically significant difference between the right and left side, a similar observation was made.

Table 4

Distribution between TMS and Keros classification ($P > 0.05$)

Keros	TMS		
Distribution of Keros and TMS classification			
Right			
Type	I	II	III
I	155	0	0
II	33	0	0
III	0	0	0
Left			
I	153	0	0
II	35	0	0
III	0	0	0

TMS, Thailand-Malaysia-Singapore.

Table 5

Distribution between Gera and TMS classification ($P > 0.05$)

TMS	Gera		
Distribution of Gera and TMS classification			
Right			
Type	I	II	III
I	2	145	41
II	0	0	0
III	0	0	0
Left			
I	2	159	27
II	0	0	0
III	0	0	0

TMS, Thailand-Malaysia-Singapore.

Table 6

Distribution between Keros and Gera's classification.

Keros		Gera	
Distribution of Keros and Gera classification			
Right			
Type	I	II	III
I	0	116	39
II	2	29	2
III	0	0	0
Left			
I	2	126	25
II	0	33	2
III	0	0	0

Right side ($P < 0.05$), Left side ($P = 0.2$).

Gera *et al.*[11] proposed a classification of the angle formed by the LLCP and the horizontal plane passing through the cribriform plate. They classified the angle into class I (> 80°), class II (45°–80°), and class III (< 45°) based on 190 CT scans. The most common anatomic variation was Keros type 2 (64.7% of cases), followed by Keros type 1 (20% of cases) and Keros type 3 (15.3% of cases). No significant differences in the distribution of Keros classification among males and females were found.

In our study, Class II was observed on the right side of 145 individuals (77.12%) and 159 (84.57%) on the left side, while Class III was observed on the right side of 32 individuals (22.34%) and 27 (14.36%) on the left side. Class, I was observed on the right side of two individuals (0.05%) and the left side of two (1.06%) individuals. In conclusion, class II was the commonest type, and type I was the rarest type.

Baharudin *et al.*[12] In their study, proposed a new radiological classification called the TMS classification, which assessed the anatomical risk of anterior skull base injury using the OrF as a reference. They compared this classification with the Keros and Gera classifications and found a significant correlation between TMS and Keros classifications, but no significant correlation between Keros and Gera classifications, as well as between TMS and Gera classifications. In contrast, our study showed significant correlation between Keros and Gera classification on the right-sided measurements while no significant correlation seen between Keros and TMS classification, Gera and TMS classification and Keros and Gera classification on left-sided measurements. In addition to that, their study observed depth of the cribriform showing a strong positive correlation with OF-ER and OF-CP. The degree of angle formed by the lateral lamella of the CP and the continuation of the horizontal plane passing through the CP had a weak positive correlation with the cribriform, OF-ER, and OF-CP depth. However, in our study weak positive correlation was seen between depth of cribriform and OF-CP as well as between OF- ER and angle formed by the lateral lamella of the CP and the continuation of the horizontal plane passing through the CP. However, there was no significant correlation seen between depth of cribriform and OF-ER. Similarly, no significant correlation of OF- CP and depth of cribriform with angle formed by the lateral lamella of the CP and the continuation of the horizontal plane passing through the CP was seen in our study. Our study's findings differed from Baharudin and colleagues' study in terms of the prevalence of Keros classifications. While their study showed Keros type 2 as the most common, followed by Keros type 1, and no Keros type 3, our study observed Keros type 1 as the most prevalent, followed by Keros type 2, with no Keros type 3. Our study also showed class I to be the rarest type, in contrast to their study where class III was the rarest type. According to the TMS classification, our study only observed type 1 in all subjects, similar to the prevalence reported by Baharudin and colleagues

The study included patients aged 18 and above who underwent CT PNS and CT head. It excluded patients with ethmoidal roof, anterior skull base, and medial wall of orbit pathology. The study did not account for variations in skull shape and morphology for measuring OF depth. Suboptimal images were discarded, and the study did not identify individuals with class III Kero's classification or TMS classification. If the sample size was larger, further variations could be observed. Although the study population closely matches the demographic of the general population, a larger sample size would have enhanced the external validity of the study.

Conclusion

This study investigated anatomical variations and Keros classification prevalence in paranasal sinus anatomy. OF depth and cribriform plate's lateral lamella showed significant individual variability. Different studies reported varying Keros prevalence, highlighting the need for preoperative imaging in surgical planning. Alternative classifications like Gera's and TMS also exhibited distinct prevalence rates. The findings emphasize the importance of understanding these anatomical variations for endoscopic nasal surgeries.

Ethical approval

We have conducted an ethical approval base on the Declaration of Helsinki with registration research at the Institutional Review Committee (IRC) of the Institute of Medicine (IOM), Tribhuvan University, Nepal.

Reference number: 236/(6-11)E^2 /077/078.

Consent

Written informed consent was obtained from the patient for the publication of this case report and the accompanying images. A copy of the written consent is available for review by the Editor-in-chief of this journal on request.

Sources of funding

None.

Author contribution

S.K.: conceptualization, as mentor and reviewer for this original article and for data interpretation. R.R.K.: as mentor and reviewer for this original article and for data interpretation. M.A.A.: conceptualization and reviewer for this case. S.S.: reviewer and data interpretation. P.G.: contributed in performing literature review and editing. All authors have read and approved the manuscript.

Conflicts of interest disclosure

The authors declare that they have no financial conflict of interest with regard to the content of this report.

Research registration unique identifying number (UIN)

1. Name of the registry: researchregistry.com.
2. Unique identifying number or registration ID: researchregistry9260.
3. Hyperlink to your specific registration (must be publicly accessible and will be checked): https://www.researchregistry.com/browse-the-registry#home/registrationdetails/64aece30a3a3f10027a3b9fa/.

Guarantor

Shailendra Katwal is the person in charge of the publication of our manuscript.

Data availability statement

Datasets generated during the current study will be available upon reasonable request.

Provinence and peer review

Not commissioned, externally peer-reviewed.

References

[1] Homsi MT, Gaffey MM. Sinus Endoscopic SurgeryHigh-risk areas in endoscopic sinus surgery and prevention of complications. in: Ohnishi T, Tachibana T, Kaneko Y, *et al*. Ed. Laryngoscope 1993;103:1181–1185.
[3] Cumberworth VL, Sudderick RM, Mackay IS. Major complications of functional endoscopic sinus surgery. Clin Otolaryngol Allied Sci 1994;19:248–53.
[4] Dessi P, Moulin G, Triglia JM, *et al*. Difference in the height of the right and left ethmoidal roofs: a possible risk factor for ethmoidal surgery. Prospective study of 150 CT scans. J Laryngol Otol 1994;108:261–2.
[5] Souza SA, Souza MMA de, Idagawa M, *et al*. Computed tomography assessment of the ethmoid roof: a relevant region at risk in endoscopic sinus surgery. Radiol Bras 2008;41:143–7.
[6] Freedman HM, Kern EB. Complications of intranasal ethmoidectomy: a review of 1,000 consecutive operations. Laryngoscope 1979;89:421–34.
[7] Keros P. [On the practical value of differences in the level of the lamina cribrosa of the ethmoid]. Z Laryngol Rhinol Otol 1962;41:809–13.
[8] Anderhuber W, Walch C, Fock C. [Conuration of ethmoid roof in children 0-14 years of age]. Laryngorhinootologie 2001;80:509–11.
[9] Başak S, Karaman CZ, Akdilli A, *et al*. Evaluation of some important anatomical variations and dangerous areas of the paranasal sinuses by CT for safer endonasal surgery. Rhinology 1998;36:162–7.
[10] Stankiewicz JA, Lal D, Connor M, *et al*. Complications in endoscopic sinus surgery for chronic rhinosinusitis: a 25-year experience. Laryngoscope 2011;121:2684–701.
[11] Gera R, Mozzanica F, Karligkiotis A, *et al*. Lateral lamella of the cribriform plate, a keystone landmark: proposal for a novel classification system. Rhinology 2018;56:65–72.
[12] Abdullah B, Chew SC, Aziz ME, *et al*. A new radiological classification for the risk assessment of anterior skull base injury in endoscopic sinus surgery. Sci Rep 2020;10:4600.
[13] Shama S, Montaser M. Variations of the height of the ethmoid roof among Egyptian adult population: MDCT study. Egypt J Radiol Nucl Med 2015;46.
[14] Bista M, Maharjan M, Kafle P, *et al*. Computed tomographic assessment of lateral lamella of cribriform plate and comparison of depth of olfactory fossa. JNMA J Nepal Med Assoc 2010;49:92–5.
[15] Babu AC, Nair MRPB, Kuriakose AM. Olfactory fossa depth: CT analysis of 1200 patients. Indian J Radiol Imaging 2018;28:395–400.
[16] Dasar U, Gokce E. Evaluation of variations in sinonasal region with computed tomography. World J Radiol 2016;8:98–108.
[17] Francies O, Makalanda L, Paraskevopolous D, *et al*. Imaging review of the anterior skull base. Acta Radiol Open 2018;7:2058460118776487.
[18] Cuschieri S. The STROBE guidelines. Saudi J Anaesth 2019;13(Suppl 1):S31–4.
[19] Mathew G, Agha R, Albrecht J, *et al*. STROCSS 2021: Strengthening the reporting of cohort, cross-sectional and case-control studies in surgery. Int J Surg 2021;96:106165.
[20] Erdogan S, Keskin IG, Topdag M, *et al*. Ethmoid roof radiology; analysis of lateral lamella of cribriform plate. Otolaryngol Pol 2015;69:53–7.
[21] Elwany S, Medanni A, Eid M, *et al*. Radiological observations on the olfactory fossa and ethmoid roof. J Laryngol Otol 2010;124:1251–6.
[22] Mishra S, Chhetri ST, Pant AR, *et al*. Prevalence of dangerous ethmoid in a tertiary center in eastern Nepal. JNMA J Nepal Med Assoc 2019;57:311–4.
[23] Costa ALF, Paixão AK, Gonçalves BC, *et al*. Cone beam computed tomography-based anatomical assessment of the olfactory fossa. Int J Dent 2019;2019:4134260.
[24] Moradi M, Dalili B. Variations of ethmoid roof in the Iranian Population—a cross sectional study. Iran J Otorhinolaryngol 2020;32:169.